
8 Discrete growth models

In this chapter, we describe a few models that have had a key impact on our knowledge about specific aspects of interface roughening. Due to intractable mathematical difficulties, numerical methods are commonly used to determine the scaling exponents for systems with $d > 1$. Most growth models originate from specific physical or biological problems, and only recently have been investigated using the methods described in this book.

8.1 Ballistic deposition

The ballistic deposition model introduced in Chapter 2 is the simplest version – termed the nearest-neighbor (NN) model because falling particles stick to the first nearest neighbor on the aggregate. If we allow particles to stick to a diagonal neighbor as well, we have the next-nearest neighbor (NNN) model (Fig. 8.1). Since the nonlinear term is present for both models ($\lambda \neq 0$), the scaling properties for both models are described by the nonlinear theory. These two models therefore belong to the same universality class, since they share the same set of scaling exponents, α , β , and z . Their non-universal parameters, however, are different. For example, for the velocity v_0 (see (A.13)), we find $v_0 = 2.14, 4.26$ for the NN and NNN models, respectively. The coefficient λ of the nonlinear term differs as well, with $\lambda = 1.30, 1.36$, respectively [249].

The origin of the nonlinear term in the model is the lateral sticking rule, leading to the presence of voids. If we now tilt the interface, the resulting aggregate becomes more porous, with an increasing number of voids (Fig. 8.2). The formation of voids increases the growth velocity of the interface, since with the same number of deposited particles the

mean height increases faster. Therefore a larger λ term is generated for the tilted case.†

8.2 Eden model

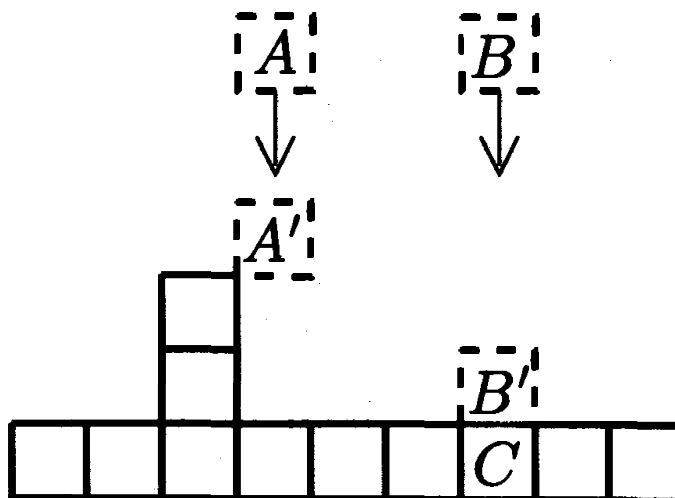
A classic growth model was introduced in 1961 by M. Eden as a model for the formation of cell colonies, such as bacteria or tissue cultures [111]. The model is defined as follows. Consider a lattice and place a seed particle at the origin. A new particle is added on any randomly-chosen perimeter site of the seed, forming thereby a two-site cluster. When iterated, the Eden model generates a cluster with a compact overall shape, but with a rough perimeter. Due to the slight anisotropy of the lattice, the roughly circular cluster is slightly distorted and resembles a diamond for a large enough number of particles [134, 178, 229, 310].

To study the interface properties of the model, it is convenient to start the growth from an entire line of seeds instead of from a single seed (Fig. 8.3). There are three versions of the Eden model, which differ in the microscopic rule of choosing the growing site [207], and result in different crossover behavior. Versions A and B have strong finite-size effects, while better scaling is found for version C. Determination of the scaling exponents can be facilitated by taking into account the 'intrinsic width' according to (A.16) [485].

Moreover, the intrinsic width can be decreased by using *noise reduction* techniques [223, 347, 348, 349, 435, 438], in which a counter is

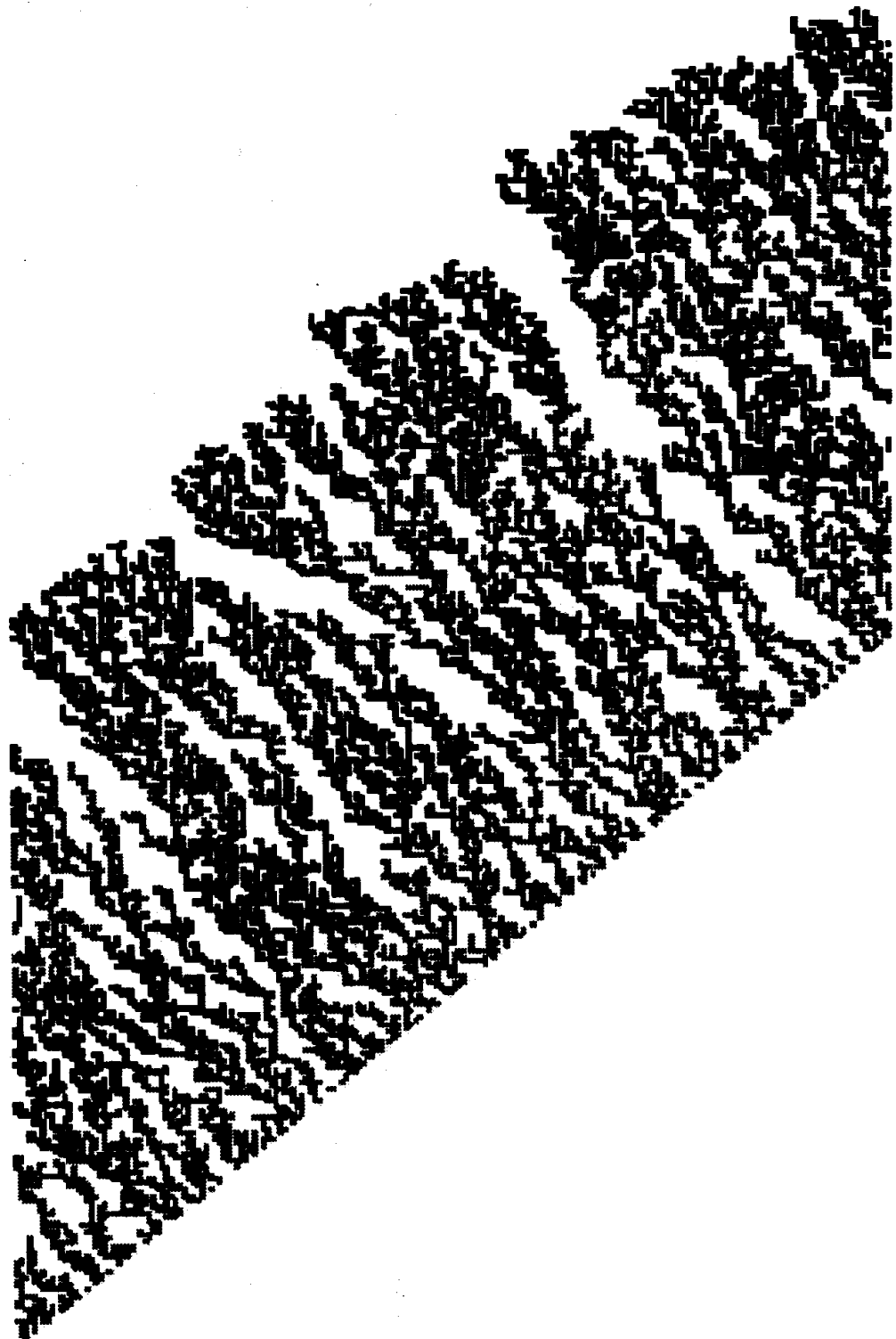
† Two numerical recipes – measurement of λ and corrections due to an intrinsic width – which are useful for following the details of this chapter, are discussed in Appendix A.

Figure 8.1 The ballistic deposition model with the next-nearest neighbor (NNN) sticking rule, to be contrasted with the NN sticking rule of Fig 2.1. Particle A sticks to the first site along its trajectory which has an occupied *next-nearest* neighbor, which is position A' . Similarly, particle B is deposited on the top of particle C.



used to record how many times a given growth site is chosen randomly from the available ones. The site is occupied only when the counter reaches a prescribed value s , called the noise reduction parameter; $s = 1$ reduces to the original model, while when $s \rightarrow \infty$ the growth is eventually deterministic. Noise-reduction algorithms allow a more

Figure 8.2 A ballistic deposition cluster generated by the NN model using a tilted substrate. A total of 16 000 particles was deposited (slope $m = 1$). Comparing with Fig. 2.2, one can see that the tilted substrate makes the aggregate grow faster, increasing the size and number of voids in the bulk.



reliable estimation of the exponents, and verify the validity of the scaling relation (6.13) [486].

The scaling properties are now believed to be described by the KPZ equation. Early simulations established $\alpha \approx 0.5$ for $d = 1$, in accord with the KPZ predictions. In higher dimensions, however, strong crossover effects give results scattered between 0.2 and 0.4 for $d = 2$ and between 0.08 and 0.33 for $d = 3$. Representative results are summarized in Tables 8.1 and 8.2.

8.3 Solid-on-solid models

Appendix A discusses the fact that many models display pronounced effects of ‘corrections-to-scaling’. One class of models, collectively called solid-on-solid (SOS) models, has been introduced in order to minimize these corrections. The SOS models (a) consider a single-valued interface, i.e., do not allow overhangs, and (b) limit the height difference between neighboring sites and thus eliminate large slopes. In this section, we discuss the two SOS-type models that have contributed most to our knowledge by providing extremely accurate values of the scaling exponents in higher dimensions.

8.3.1 Single-step model

The single-step model is useful because one can obtain some of its parameters analytically by, e.g., mapping it to an Ising model [312,

Figure 8.3 The three versions of the Eden model. (a) In version A, a particle is added with equal probability to any unoccupied site (dotted sites) adjacent to the surface (shaded sites). (b) In version B, a bond (dotted segments) linking an occupied site on the cluster with an empty perimeter site is chosen with equal probability. In version C, not shown, an occupied site on the surface is chosen with equal probability, and the new particle is added, with equal probability, to any of the empty sites adjacent to the chosen occupied particle. The three versions produce interfaces that differ microscopically, but belong to the same universality class.

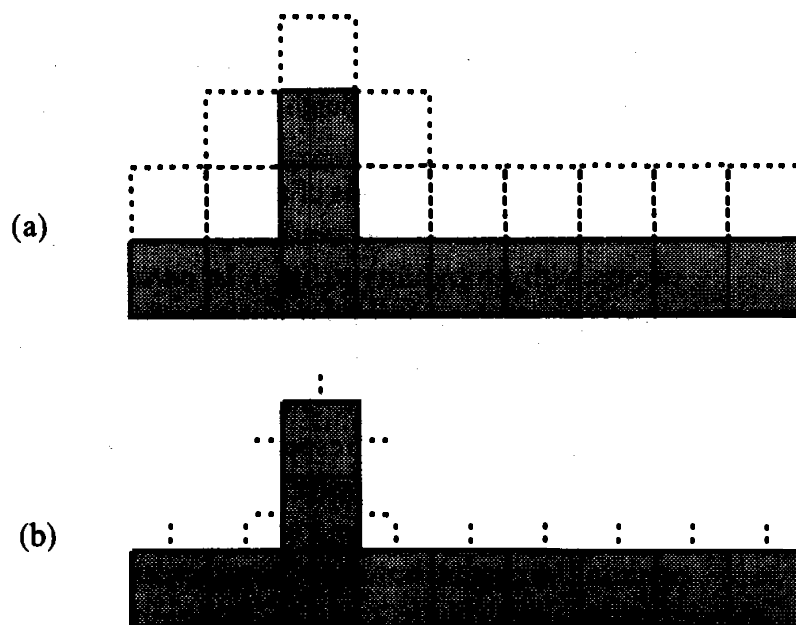


Table 8.1 *Numerical results for exponents in the strong coupling limit, for the case $d = 1$.*

Model	α	β	z	Reference
Ballistic	0.42	0.30		[124]
Ballistic	0.47	0.30		[312]
Ballistic		0.33		[20]
Eden	0.50			[124]
Eden			1.55	[372]
Eden	0.50	0.30		[206]
Eden	0.50	0.30		[310]
Eden	0.51	0.32		[501]
Single Step	0.5	0.33		[312]
Single Step			1.57	[373]
RSOS	0.5	0.33		[231]
RSOS	0.489	0.332		[2]
PNG		0.33		[252]
KPZ	0.5	0.33		[155]
KPZ		0.330		[330]

373]. The model, illustrated in Fig. 8.4, is defined as follows. At time $t = 1$ the interface has a grooved shape, with height $h(2i) = 0$ and $h(2i + 1) = 1$, where $i = 0, \dots, L/2$. Growth occurs with a probability p_+ at each local minimum, resulting in $h_i \rightarrow h_i + 2$. The interface can decrease its height ('desorption') at site i , if that site is a local maximum. Desorption occurs at local maxima with probability p_- , resulting in $h_i \rightarrow h_i - 2$. The fact that we always choose the local minima (maxima) to grow (desorb) guarantees that at any stage of the growth process the height difference between two neighboring sites must be exactly unity.

There are two methods of updating the model. In *sequential updating* a site on the interface is randomly selected, and growth (or desorption) occurs with probability p_+ (p_-). In *parallel updating*, all eligible growth sites (i.e., all local minima) grow with probability p_+ simultaneously, and all eligible desorption sites desorb with probability p_- . It is possible to separate the lattice into two sublattices (formed by odd and even lattice sites, respectively), and perform the updating on a parallel or vector computer. This makes the simulation of the model very effective. The scaling exponents are independent of the way we update the model, but some parameters may depend on the simulation method.

Table 8.2 Numerical results for the exponents in the strong coupling regime, for $d > 1$.

Model	d	α	β	z	Reference
Ballistic	2+1	0.33	0.24		[312]
Ballistic	2+1	0.3	0.22		[20]
Ballistic	2+1	0.35	0.21		[120]
Eden	2+1	0.20			[206]
Eden	2+1	0.33	0.22		[486]
Eden	2+1	0.39	0.22		[106]
Single Step	2+1	0.36		1.58	[312]
Single Step	2+1	0.375		1.63	[276]
Single Step	2+1	0.385	0.240		[131]
RSOS	2+1	0.40	0.25		[231]
KPZ	2+1	0.18	0.10		[71]
KPZ	2+1	0.24	0.13		[155]
KPZ	2+1	0.39	0.25		[4]
KPZ	2+1		0.240		[330]
Eden	3+1	0.08			[206]
Eden	3+1	0.24	0.146		[486]
Eden	3+1	0.22	0.11		[106]
Single Step	3+1	0.30	0.180		[131]
RSOS	3+1		0.20		[231]
RSOS	3+1	0.294	0.180	1.709	[2]
KPZ	3+1		0.17		[330]
RSOS	4+1		0.16		[231]
RSOS	4+1	0.254	0.139		[2]
RSOS	5+1		≥ 0.107		[2]
RSOS	6+1		≥ 0.10		[2]
RSOS	7+1		≥ 0.08		[2]

Kinetic Ising model – To map the single-step model to a kinetic Ising model, we observe that the interface properties can be described in terms of a set of Ising variables $\{s\} = \{s_1 s_2, \dots, s_L\}$, where

$$s_i \equiv h(i) - h(i-1) = \pm 1. \quad (8.1)$$

At $t = 0$ we have ‘antiferromagnetic’ ordering – i.e., up and down spins alternate (Fig. 8.4). Growth can occur if two spins (s_i, s_{i+1}) have

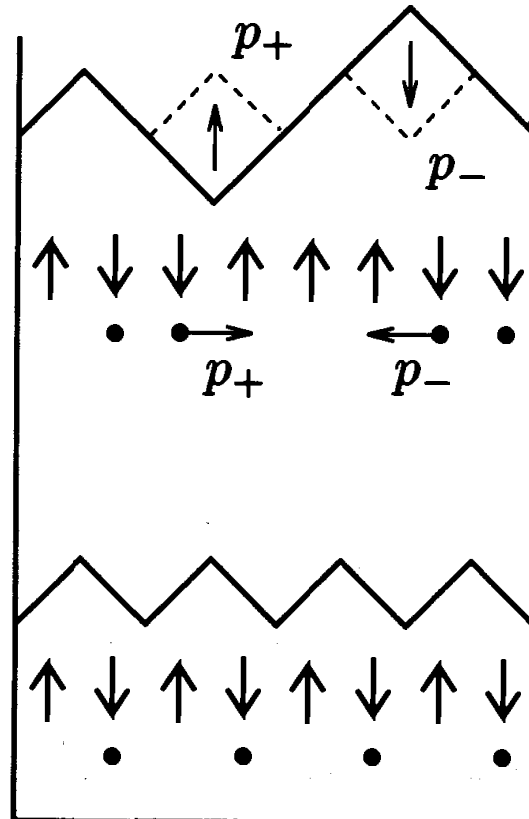
a $(-+)$ configuration; growth of the interface at site i exchanges the value of the two spins with a probability $p_+ = 1/2$. The transition $(-+) \rightarrow (+-)$ conserves the total 'magnetization' of the system. Similarly, desorption occurs with probability p_- , resulting in the transition $(+-) \rightarrow (-+)$.

Lattice gas model – The single-step model can be mapped to a lattice gas if we replace every surface element of slope (-1) with a hard core particle, and every element with slope $(+1)$ with a hole (Fig. 8.4). Thus initially we have $L/2$ particles, placed at every second lattice site. A growth process corresponds to rightward motion of the corresponding particle, and desorption to leftward motion. In the lattice gas model, particles move to the right (left) with a probability p_+ (p_-), with the restriction that only one particle can occupy each site at any given moment. This condition corresponds to the height-difference restriction in the original growth model.

Nonlinear term – If the model is described by the nonlinear theory, an overall tilt should change the velocity of the interface (see Appendix A). The interface velocity is given by the relation

$$v = 2(\Pi_+ p_+ - \Pi_- p_-), \quad (8.2)$$

Figure 8.4 Schematic representation of the single-step model and the equivalent Ising and lattice gas models. The initial smooth configuration (bottom) is a grooved surface, equivalent to alternating Ising spins, or to the presence of a particle at every second site (lattice gas). At a later time, we have a rough interface (top), corresponding to a random distribution of up-down spins or diffusing particles.



where Π_+ (Π_-) is the probability of choosing a site eligible for growth (desorption), and the factor 2 arises from the fact that every growth process increases the interface height by 2. For the untilted interface, the number of eligible growth sites equals the number of sites eligible for desorption, so $\Pi_+ = \Pi_-$. In the case $p_+ = p_-$, the interface does not grow. There is an up-down symmetry in h – i.e., desorption and deposition are equally probable. Hence, following the discussion of symmetry principles in § 5.2, the model must be described by the EW equation.

Suppose we elevate the right side of the interface by k lattice spacings, thereby generating an overall tilt of slope $m \equiv k/L$. In the spin representation this will increase (decrease) the initial number of up (down) spins, and

$$N_+ = \frac{L}{2} + \frac{mL}{2}, \quad N_- = \frac{L}{2} - \frac{mL}{2}. \quad (8.3)$$

One essential property of the kinetic Ising model is that in its steady state all configurations $\{s_i\}$ are equivalent. The probability Π_+ of finding a pair $(-+)$ eligible for growth can be calculated as follows. The probability of finding a $(+)$ spin is $N_+/(N_+ + N_-)$, and the probability of finding *next to it* a $(-)$ spin is $N_-/(N_+ + N_-)$. Thus the probability of finding a $(-+)$ combination is

$$\Pi_+ = \frac{N_+ N_-}{(N_+ + N_-)^2}, \quad (8.4)$$

which is the probability of finding a site eligible for growth. The same expression also gives Π_- .

Using (8.2)–(8.4), we thereby obtain for the tilt-dependent velocity

$$v(m) = \frac{(p_+ - p_-)}{2} (1 - m^2) \quad (8.5)$$

which, combined with (A.13), gives the coefficient of the nonlinear term in the KPZ equation

$$\lambda = -(p_+ - p_-). \quad (8.6)$$

This relation expresses quantitatively the fact that for $p_+ = p_-$, the nonlinear term vanishes, and the model is described by the Edwards–Wilkinson equation, (5.6). A second observation is that the growing interface ($p_+ > p_-$) has $\lambda < 0$, so the local velocity decreases with the local slope.

Scaling exponents – A simple argument can provide the roughness exponent as well [312]. In equilibrium, all configurations are equally

probable, so neighboring spins are uncorrelated, $\langle s_i s_j \rangle = \delta_{ij}$. The height of the interface at site k is

$$h_k = \sum_{i=1}^k s_i + h_1. \quad (8.7)$$

These properties are reminiscent of Brownian motion: the trace of a Brownian particle is given by the sum of uncorrelated random numbers as the particle performs a random walk of k steps, each of length ± 1 . Hence the roughness exponent of the interface is $\alpha = 1/2$, which coincides with the predictions of both the EW and KPZ equations.

The previous argument can be used in the equilibrium situation, for which the interface does not grow and $p_+ = p_-$. It is also applicable to the moving interface as well, which is a nonequilibrium problem [312]. The equilibrium state of the kinetic Ising model corresponds to the stationary (saturated) state of the nonequilibrium growth model. While both the KPZ and EW theories predict the same roughness exponent, $\alpha = 1/2$, they predict different dynamic exponents z .

Generalizations of single-step models to $d > 1$ provide the first systematic study of conjectures (7.20) and (7.21) [131, 441]. For $d > 1$, $d + 1$ -dimensional hypercubes are deposited on (or desorbed from) a d -dimensional interface. The rate of deposition (or desorption) is p_+ (or p_-). If deposition is balanced with desorption, one can expect exponents predicted by the linear theory [see (5.16)].

Such tuning of the deposition and desorption rates allows us to systematically study crossover effects, and thus to locate the scaling region. One source of deviation of the effective roughness exponent from its asymptotic value is a crossover from the scaling behavior of the linear equation to the nonlinear one, if the value of the effective coupling constant $g \sim D\lambda^2/\nu^3$ is small. For parallel updating, the choice $p_+ = 1/2$ and $p_- = 0$ maximizes this quantity, while for sequential updating, $p_+ = 1$ and $p_- = 0$ according to (8.6). Large Monte-Carlo simulations incorporating corrections-to-scaling give exponents different from the predictions of (7.20) and (7.21) (see also Fig. 7.6).

8.3.2 Restricted solid-on-solid model

The restricted SOS model, introduced by Kim and Kosterlitz (KK), permitted the first systematic investigation of growth exponents for higher dimensions [231]. The KK growth algorithm randomly selects a site on a d -dimensional interface, and increases the height of the interface by one, $h_i \rightarrow h_i + 1$, provided that at every stage of

growth the restricted solid-on-solid condition $|\Delta h| = 0, 1$ is fulfilled between the selected and the neighboring sites.[†] The model exhibits very good scaling properties, without noticeable intrinsic width or corrections-to-scaling. Tilt-dependent velocity measurements reveal that the coefficient of the nonlinear term is negative: $\lambda = -0.75$ [249].

KK studied their model for $d \leq 4$. They concentrated on the determination of the exponent β , because this exponent describes the early time behavior of the interface width and so does not require the saturation of the system (which for large systems is very time consuming). The results, summarized in Tables 8.1 and 8.2, led KK to conjecture that the dimension dependence of the exponents is given by (7.21). By using a fitting *Ansatz* from the correlation function, Ala-Nissila *et al.* were able to obtain more reliable estimates of the exponents [2]. Their values are systematically larger than those given by (7.21), and are in agreement with the $d > 1$ hypercube-stacking simulations mentioned in the previous section.

8.4 Propagation of interfaces in the Ising model

When the temperature is sufficiently low, a well-defined interface develops between the up and down spins in a simple Ising model during the growth of the stable phase at the expense of the unstable phase. For the Ising model in a field H , Eq. (7.1) is replaced by

$$\mathcal{H} = -J \sum_{\langle ij \rangle} s_i s_j - H \sum_i s_i. \quad (8.8)$$

Here $\langle ij \rangle$ denotes a sum over the nearest-neighbor pairs, J the nearest-neighbor coupling constant, and H the external field. The system follows nonconservative dynamics, such as the one proposed by Metropolis in which spins are flipped with a probability

$$P(s \rightarrow s') \propto \exp \left(-\frac{\mathcal{H}(s') - \mathcal{H}(s)}{k_B T} \right). \quad (8.9)$$

We prepare our system such that there is a straight interface separating two domains, one with spins up and the other with spins down. We have one stable domain (with spins oriented parallel to H) and one unstable domain (spins antiparallel to H) on decreasing the temperature to below the critical temperature. The stable phase grows, making the interface advance at the expense of the unstable one. The properties of this evolving interface can be described by the

[†] In general, one can assume $|\Delta h| = 0, 1, \dots, k$ without changing the growth exponents, but most of the simulations are performed for the simplest case $k = 1$.

KPZ equation [105, 254]. An unwanted effect that can disturb the identification of the interface is the nucleation and droplet growth of the stable phase in the bulk of the unstable phase. These 'islands' eventually coalesce with the growing interface, changing its geometrical structure. In simulations, this effect can be eliminated by allowing spins to flip only in the vicinity of the interface, thus neglecting the dynamics of the bulk.

8.5 Numerical integration of the KPZ equation

So far, we have concentrated on the determination of the exponents of the nonlinear theory using discrete models that are believed to belong to the KPZ universality class. Despite the presented analytical and numerical evidence that these models have a nonzero nonlinear term, the reader might reasonably doubt our claim that they can be described using the KPZ equation, or, conversely, that the KPZ equation predicts the same exponents as the models. The situation is clear in one dimension, where exact values of the KPZ exponents can be determined analytically and their values coincide with the numerical results, but is less clear in higher dimensions.

An alternative proof might be possible if we could obtain the scaling exponents directly from the growth equation. For these reasons, many groups have tried to obtain the scaling exponent by integrating numerically the KPZ equation [4, 71, 155, 329, 330]. Early investigations have found very small values of β in two dimensions, compared to the results provided by discrete models. Later works have reported agreement with the lattice models [4, 329, 330]. In addition, a very detailed investigation by Moser *et al.* [329, 330] has produced evidence of a phase transition between the smooth and rough phase in $d = 3$.

To integrate numerically the KPZ equation, one must discretize the continuum equation, (6.4). This is done by using a forward-backward difference method on a cubic grid with a lattice constant Δx , and the Euler algorithm with time increments Δt . Denoting the basis vectors by $\mathbf{e}_1, \mathbf{e}_2, \dots, \mathbf{e}_d$, and labeling the grid points by \mathbf{n} , we find for the discretized growth equation

$$\begin{aligned}
 h(\mathbf{x}, t + \Delta t) = & h(\mathbf{x}, t) + \\
 & \frac{\Delta t}{(\Delta \mathbf{x})^2} \sum_{i=1,d} (\nu [h(\mathbf{x} + \mathbf{e}_i, t) - 2h(\mathbf{x}, t) + h(\mathbf{x} - \mathbf{e}_i, t)] \\
 & + (1/8)\lambda [h(\mathbf{x} + \mathbf{e}_i, t) - h(\mathbf{x} - \mathbf{e}_i, t)]^2) + \sigma(12\Delta t)^{1/2}\eta(t). \quad (8.10)
 \end{aligned}$$

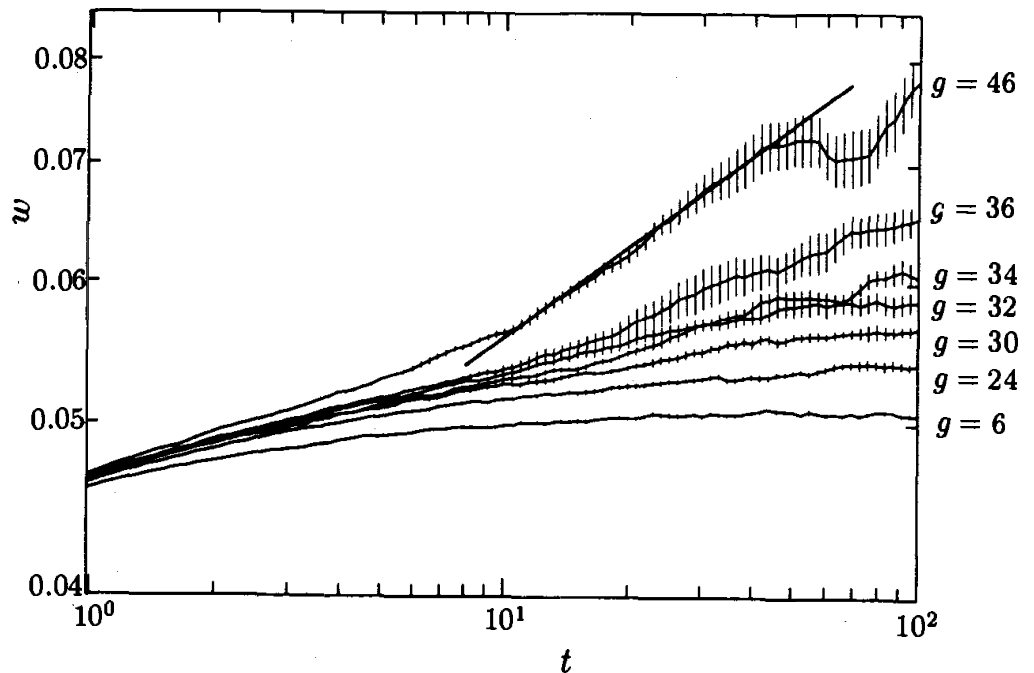
Here $\sigma^2 \equiv 2D/(\Delta x)^d$, and the random numbers η are uniformly distributed between $-1/2$ and $1/2$. For practical purposes it is useful to use the dimensionless variables $\tilde{h} \equiv h/h_0$, $\tilde{t} \equiv t/t_0$ and $\tilde{x} \equiv x/x_0$, where the natural units can be obtained from the combination of the coefficients of the growth equation $h_0 = v/\lambda$, $t_0 = v^2/\sigma^2\lambda^2$, and $x_0 = (v^3/\sigma^2\lambda^2)^{1/2}$, while the dimensionless coupling constant is given by $g = (\Delta\tilde{x})^d/2$.

Simulating the KPZ equation in these dimensionless parameters gives $\beta = 0.330 \pm 0.004$, in good agreement with the exact result $1/3$ [330]. For two dimensions, the same method gives $\beta = 0.240 \pm 0.005$, coinciding with the value found in the SOS models (Table 8.2).

The results obtained for three dimensions are particularly interesting. As can be seen in Fig. 8.5, at $g^* \approx 32$, there is a qualitative change in the curves. The upward trend of the curves for large coupling constant can be interpreted as a sign of kinetic roughening, g^* representing the transition point between smooth and rough phases. Further studies on the ensemble fluctuations also indicate the presence of a transition at g^* . These results are in good agreement with the predictions of the dynamic RG analysis, that a smooth-to-rough transition is possible in dimensions higher than two (see §7.4).

Figure 8.5 Time dependence of the width for the KPZ equation with $d = 3$.

The qualitative change in the curves at $g^* = 32$ indicates the possibility of a morphological phase transition from the smooth phase ($g < 32$) to roughening ($g > 32$). (After [330]).



8.6 Discussion

There are various reasons for introducing a discrete growth model. A number of models are designed to faithfully mimic some natural process. In particular, the BD and Eden models were designed to simulate vapor deposition and biological growth, respectively. These models have certain limitations – e.g., they cannot provide accurate scaling exponents. To go beyond these limitations, we need models that will provide answers to specific questions. A good example is the SOS model, which does not exhibit strong corrections-to-scaling and so allows the accurate determination of scaling exponents.

Although we are not able to calculate the KPZ exponents analytically for $d > 1$, the use of discrete models does enable us to obtain good estimates of exponent values. Why is it important for us to have accurate numerical values for the exponents? First, in order to identify the universality class, we need to know the exponents. Second, when we measure an exponent experimentally, we also need to know the value of the exponent in order to determine whether the growth process is indeed described by the KPZ equation.

Suggested further reading:

[254, 304, 330]

Exercises:

- 8.1 Write a computer program that simulates the NNN ballistic deposition model, and compare the scaling of the interface width with that of the NN model.
- 8.2 Calculate λ for the NN and NNN ballistic deposition models.
- 8.3 In the BD model $\lambda > 0$, while in the SOS models $\lambda \leq 0$. In the Eden model, is λ positive or negative? Does the sign vary from version to version of this model?